Plant Biotechnology Journal

Plant Biotechnology Journal (2012) **10**, pp. 207–216 doi: 10.1111/j.1467-7652.2011.00656.x

Plant-based FRET biosensor discriminates environmental zinc levels

Joshua P. Adams[1,*], Ardeshir Adeli[2], Chuan-Yu Hsu[3], Richard L. Harkess[4], Grier P. Page[5], Claude W. dePamphilis[6], Emily B. Schultz[3] and Cetin Yuceer[3]

[1]*School of Forest Resources, University of Arkansas at Monticello, Monticello, AR, USA*
[2]*USDA-ARS, Mississippi State, MS, USA*
[3]*Department of Forestry, Mississippi State University, Mississippi State, MS, USA*
[4]*Department of Plant and Soil Sciences, Mississippi State University, Mississippi State, MS, USA*
[5]*RTI International, Atlanta, GA, USA*
[6]*Department of Biology, Pennsylvania State University, University Park, PA, USA*

Received 7 March 2011;
revised 20 July 2011;
accepted 25 July 2011.
**Correspondence* (Tel +1 870 460 1348; fax +1 870 460 1092; email adamsj@uamont.edu)

Keywords: zinc interaction, environmental monitoring, ZIP transporter, ECFP, DsRED.

Summary

Heavy metal accumulation in the environment poses great risks to flora and fauna. However, monitoring sites prone to accumulation poses scale and economic challenges. In this study, we present and test a method for monitoring these sites using fluorescent resonance energy transfer (FRET) change in response to zinc (Zn) accumulation in plants as a proxy for environmental health. We modified a plant Zn transport protein by adding flanking fluorescent proteins (FPs) and deploying the construct into two different species. In *Arabidopsis thaliana,* FRET was monitored by a confocal microscope and had a 1.4-fold increase in intensity as the metal concentration increased. This led to a 16.7% overall error-rate when discriminating between a control (1 μM Zn) and high (10 mM Zn) treatment after 96 h. The second host plant (*Populus tremula* × *Populu salba*) also had greater FRET values (1.3-fold increase) when exposed to the higher concentration of Zn, while overall error-rates were greater at 22.4%. These results indicate that as plants accumulate Zn, protein conformational changes occur in response to Zn causing differing interaction between FPs. This results in greater FRET values when exposed to greater amounts of Zn and monitored with appropriate light sources and filters. We also demonstrate how this construct can be moved into different host plants effectively including one tree species. This chimeric protein potentially offers a method for monitoring large areas of land for Zn accumulation, is transferable among species, and could be modified to monitor other specific heavy metals that pose environmental risks.

Introduction

Zinc (Zn) levels can build up in the environment and adversely impact both animal and plant communities. Some extreme contaminated sites are easily identified by biota mortality or by biota exhibiting classic contamination signs (e.g. foliar chlorosis, necrosis and loss of turgor) (Ebbs *et al.*, 2002; Adams *et al.*, 2011). Nonpoint sources causing gradual metal accumulation in soil and the food chain or heterogeneity of the metal distribution can pose a larger threat because of inabilities to diagnose contamination. Realization of threats from Zn accumulation or other similar metals (i.e. heavy metals that are group IIB transition metals on the periodic table), such as cadmium, is vital for the protection of food production and soil management (Podar *et al.*, 2004). In current agricultural practices, soil sampling is a vital, widely used tool for monitoring and managing soil. While this enables identification of heavy metals, such tests are static in time and are costly across large land areas. Also, soil leaching can lead to metal movement beyond sampled areas causing sampling to miss areas of contamination (Chaney, 1993).

One approach to monitor environmental metals is to measure organism metal concentrations *in vivo* as a proxy for environmental metals. Plants have many benefits for use in this method. One benefit is that they produce large amounts of biomass that provides adequate amounts of tissue for sampling, as opposed to using microbes. Also, they are stationary and can provide large, expansive root systems allowing for nutrient acquisition from a broad area of soil. Finally, a plant that is a perennial with large ecological applicability could be selected, which would minimize the need for annual replanting and allow for implementation across an array of sites.

These benefits point to a tree species. Perennial, fast growing forest species, such as pine (*Pinus* spp.), poplar (*Populus* spp.) and willow (*Salix* spp.), all rapidly produce biomass and could be considered. For example, *Populus deltoides* Marsh. (eastern cottonwood) is the fastest growing native forest species in North America and, unlike annual species, can live for decades (Cooper and van Haverbeke, 1990). Using plant species such as these, unlike annual species, would not require the needed yearly harvesting and replanting, decreasing the intensity of management. This would be more environmentally friendly

(i.e. less runoff, pesticides, herbicides and soil alteration) and not further compound any potential environmental hazards for which the monitoring is intended. Furthermore, many of these tree species can tolerate a large range of sites including *Populus euramericana* that can be grown in field conditions at a pH range of 3–8 (DesRochers *et al.*, 2003). Because of their rapid growth, diverse site applicability and large biomass attributes, many of these tree species have already been employed in carbon sequestration efforts under the Kyoto Protocol Article 3 (Watson *et al.*, 2000) and for reclamation of heavy metal contaminated sites (Vervaeke *et al.*, 2003; Bojarczuk, 2004).

While plants, and especially tree species, can provide large sinks for various substrates, sampling tissues would still incur costs similar to soil nutrient analysis. A real-time method is potentially feasible using currently available fluorescent proteins (FPs) and genetic modification techniques. Using chimeric proteins with two different fused FPs, protein/Ca^{2+} interactions, glutamate concentrations and ribose uptake and metabolism (Miyawaki *et al.*, 1997; Lager *et al.*, 2003) have been monitored *in vitro* by the changes in fluorescent emissions resulting from protein conformational changes. Recently, this use of FP fusions has been expanded to monitor *in vivo* concentrations of glutamine, glucose and sucrose in plant roots (Chaudhuri *et al.*, 2008; Yang *et al.*, 2010).

This fluorescent resonance energy transfer (FRET) provides a means for substrate monitoring. As metal substrate interacts with the receptor, the protein conformation changes from a relaxed conformation to a tense conformation. As this occurs, the distance between the fused FPs also changes. Change in distance causes differential energy transfer between the two FPs and has been used to successfully monitor intracellular Zn (Vinkenborg *et al.*, 2009). Thus, two scenarios are (i) an excitation wavelength, with appropriate wavelength specificity, strikes the donor FP, energy transfer is spatially prohibited and emission is only detected from the donor FP and (ii) an excitation wavelength, with appropriate wavelength specificity, strikes the donor FP, energy transfer occurs between the two FPs, and emission occurs from the acceptor FP. This second scenario occurs when the two FPs are spatially close, about 30–100 angstroms (Lakowicz, 1999). As emission changes a mass across the whole tissue, spectral changes can be correlated with the respective metal/chemical changes, resulting in a real-time, continuous monitoring system.

Real-time monitoring has been absent in proposed soil health measurement methods including fungal produced crystal counts (Sanyal *et al.*, 2005) and plant phytochelatin counts (Gawel and Hemond, 2004). However, current FRET technologies have been shown to potentially fill this gap; though, such a technique has not been implemented in plant species for the intent of soil monitoring. Thus, the objective of this study is creation of a chimeric protein that is a Zn responsive/interacting protein and successfully expresses in plant species including one tree species. Using this expressed construct, Zn absorption may be monitored *in vivo* and used to deductively gauge soil health.

Results

Arabidopsis thaliana FRET activity

Seven lines of *A. thaliana* were confirmed to contain the fluorescent *Pro$_{PtZNT}$:DsRed:PtZNT:ECFP* [PRZC (Figure 1a)] construct (see Experimental procedures) via RT-PCR (Figure 1b). However, when leaf tissues were visualized, three of the lines (Lines 3, 5 and 6) responded similarly to the wild-type control showing little or no evidence of fluorescence emission beyond the background noise (Figure 1c). Lines 1, 2, 4 and 7 exhibited varying emissions, which is expected because varying phenotypes among plant lines often occur owing to the random insertion of the gene construct into the plant genome (Allen *et al.*, 1999; Li and Brunner, 2009). From these four lines, only three (Lines 1, 2 and 7) were randomly selected for further study owing to physical limitations of the study size.

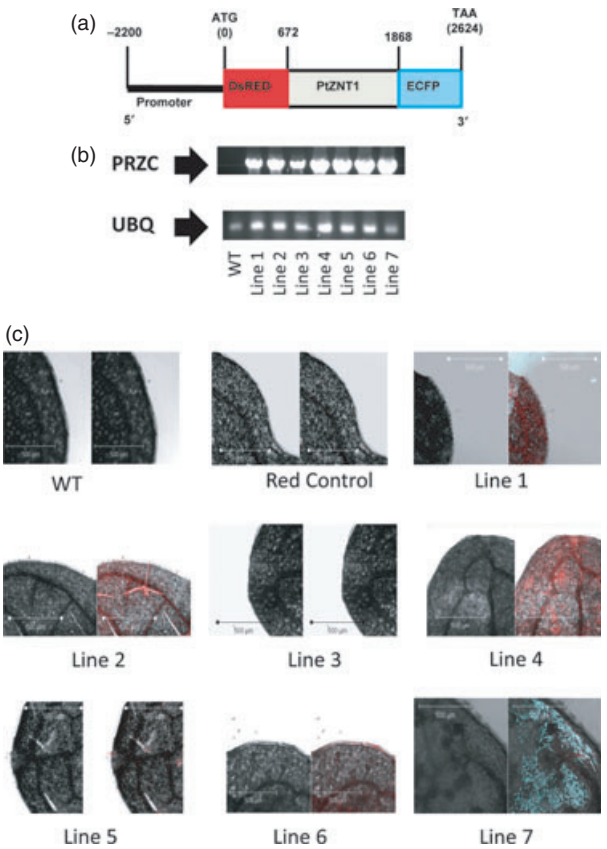

Figure 1 Fluorescent resonance energy transfer (FRET) activity in *Arabidopsis thaliana*. (a) Linear representation of the chimeric sequence [(*Pro$_{PtZNT}$:DsRed:PtZNT:ECFP* (PRZC)] which is a fusion of *Prom$_{PtZNT}$, ECFP, PtZNT* and *DsRED*. (b) Expression of PRZC was confirmed in fifth-generation lines of *A. thaliana* with RT-PCR using ubiquitin (UBQ) as an internal control baseline and a wild-type plant (WT) as a control. (c) Confirmed lines were exposed to excitation wavelengths simultaneously to test for fluorescence functionality.

In the metal-time assay, the control had no significant time or metal effects (P = 0.94 and 0.77, respectively) on FRET intensity in the model (Table S1). When plotted across time and Zn concentration, the normalized FRET intensity changed little as indicated by its flat shape and similar colour pattern (Figure 2a). Line 2 FRET was also not significantly affected by either the metal or metal-by-time effect (P = 0.21 and 0.51, respectively), indicating that FRET was unresponsive to metal concentration. Line 1 FRET was marginally affected by the time-metal interaction (P = 0.05), while Line 7 was highly significantly affected by the time-metal interaction (P = 0.001). Predicted FRET values of Line 7 plotted across a constructed time and metal matrix showed that the FRET intensity is unreliable for predictive purposes at early time points after the application of Zn treatments

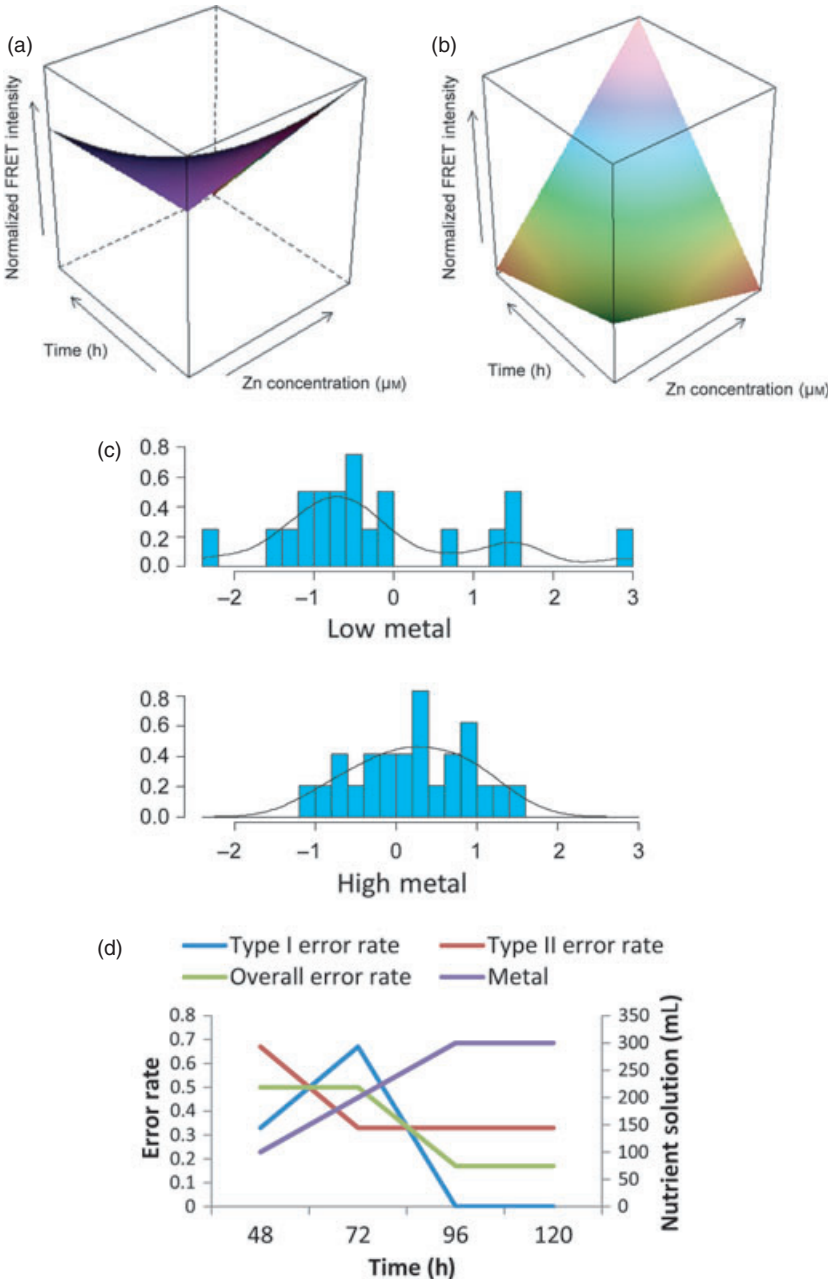

Figure 2 Effect of Zn concentrations on fluorescent resonance energy transfer (FRET) activity in *Arabidopsis thaliana* leaf tissue. Normalized FRET intensity for (a) control and (b) Line 7 was plotted three-dimensionally across time (0–144 h) and metal treatments (1 μM and 10 mM $ZnSO_4$), where FRET was indicated by both colour change and *z*-axis slope. The values from the *A. thaliana* Line 7 discriminant function were calculated and displayed in a histogram (c) for both treatments of high and low Zn where the *x*-axis was the discriminant function results on which the classification was based and the *y*-axis was the proportion of the total sampling for the assay. An independent set of plants was assayed and (d) error-rates from using the *a priori* discriminant functions were calculated for each time point (*x*-axis) and nutrient solution (secondary *y*-axis).

(Figure 2b). As time increased to 24 and 48 h, the FRET greatly increased (higher red fluorescence relative to cyan fluorescence) with the continued increases in metal exposure.

Discriminant analysis on this initial dataset for Line 7 was poor using all four of the metal concentrations [i.e. 1 μM (control), 26 μM, 1 mM and 10 mM $ZnSO_4$] as classification groups with a total posterior probability error-rate of 59%. However, further inspection of the model's confusion matrix indicated that most misclassifications occurred between the lower metal concentration treatments. Therefore, classification groups were condensed into a high/low metal classification, and the discriminate analysis was repeated. Function coefficients derived from this re-analysis (Table S2) demonstrated that greater FRET values, above an inflection point of 1.0213, were classified into the high metal exposure grouping; whereas, values below this inflection point were classified as being in the low metal exposure group. Posterior classification of this grouping produced an overall error-rate of 8.3% (Table S3). Furthermore, there were no Type II errors (concentrations classified as high that were actually low) and only 16.7% Type I errors (concentrations

classified as low that were actually high). A histogram of discriminant function results showed that FRET values from tissues under high-exposure group together tightly while low exposure FRET values do not (Figure 2c). This demonstrates an overall greater precision of classifying high-exposure plants.

When the discriminant function was used on the independent data set with high/low metal classification assumed *a priori*, miss-classifications were higher in the first two sampling periods. Overall, both the 48 and 72 h time periods had 50% miss-classification (Figure 2d). However, as the metal was continually loaded through time into the plant systems, the miss-classifications went down substantially with only 33% Type II errors and no Type I errors after 96 h. This demonstrates that using such a bio-sensor is time dependent as translocation into leaves must have time to occur. Still, after 120 h of exposure to the 10-mM Zn treatment, actual Zn accumulation in leaf tissue had 3.3-fold greater Zn compared with the 1-μM Zn treatment. This demonstrates that there is measurably greater Zn intake in a short-time period following increased Zn exposure (Table S4).

Poplar FRET activity

Four poplar lines were selected from prescreening (Figure 3a,b) and Zn accumulation in their leaves after 120 h in the 10-mM Zn treatment had 4.7-fold greater Zn compared with the 1-μM Zn treatment across lines (Table S4). In this assay, there was a significant metal effect on FRET response (P = 0.046 and 0.035, respectively for Lines 1 and 3) in their general linear model. When the model was projected across time and metal gradient, Line 3 had a FRET response (Figure 4a) similar, but compressed in magnitude [i.e. the z-axis (labelled Normalized FRET intensity)], to that observed in *A. thaliana* Line 7 (Figure 2b). Also, the initial use of the *A. thaliana* Line 7 functions was not successful in discriminating between poplars exposed to the same high/low Zn treatments. The *A. thaliana* model classified all poplar samples as being exposed to the lower, control Zn treatment and the original *A. thaliana* model spanned a different time scale. Thus, a different function was used, which included a time component, and coefficients were derived specifically for poplar. A histogram of the resulting values (Figure 4b) showed

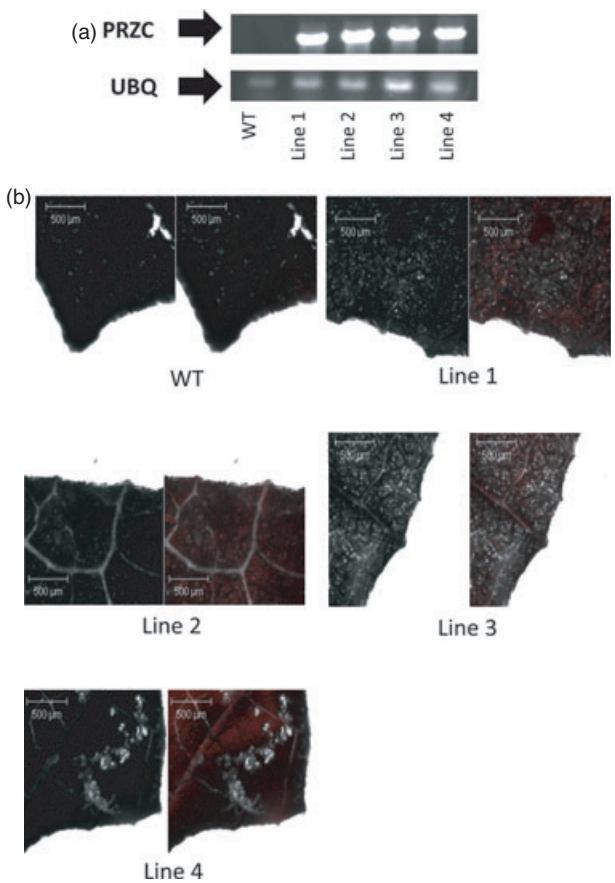

Figure 3 Fluorescent resonance energy transfer (FRET) activity in poplar (*Populus tremula* × *Populus alba*). (a) *Pro$_{PtZNT}$:DsRed:PtZNT:ECFP* expression was confirmed via RT-PCR in propagated lines with each line's ubiquitin (*UBQ*) expression used as an internal control baseline and a wild-type plant (WT) as a control. These confirmed lines were (b) exposed to cyan and red excitation wavelengths simultaneously to test for fluorescence functionality.

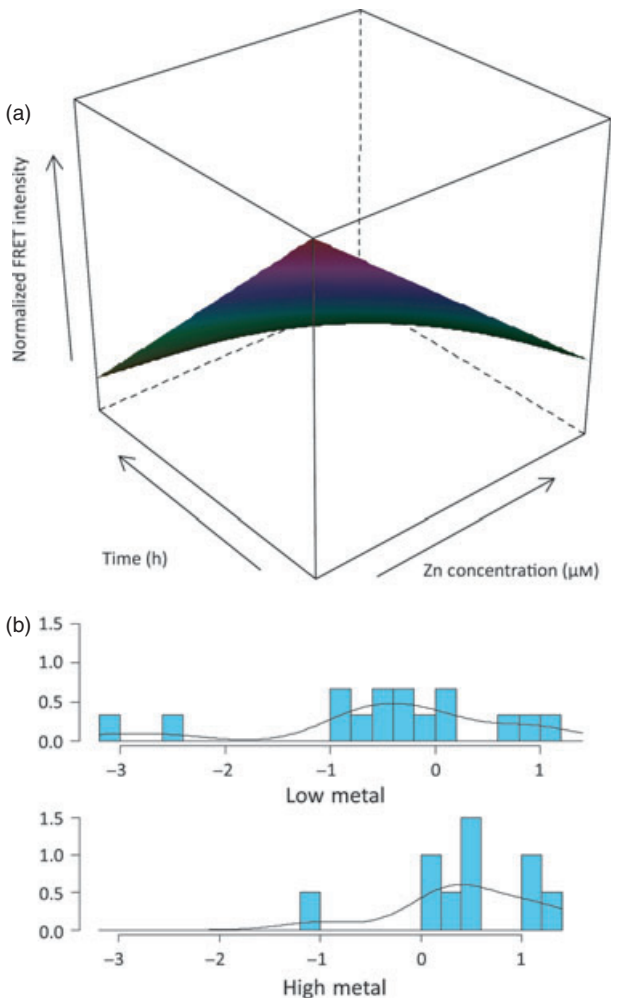

Figure 4 Effect of Zn concentrations on fluorescent resonance energy transfer (FRET) activity in poplar leaf tissue. (a) Normalized FRET intensity for Line 3 was plotted three-dimensionally across time (0–144 h) and metal treatments (1 μM and 10 mM $ZnSO_4$), where FRET was indicated by both colour change and z-axis slope. The values from the poplar Line 3 discriminant functions were calculated and displayed in a histogram (b) for both treatments of high and low Zn where the x-axis was the discriminant function results on which the classification was based and the y-axis was the proportion of the total sampling for the assay.

a clear difference from the *A. thaliana* functions (Table S2). Values resulting from the poplar function did not cluster very tightly, which may have impeded classification success (Figure 4b). Based on an average 3-day exposure, the inflection point for classification was approximately 8.0 where FRET values greater than this were classified as being exposed to high metal concentrations. Posterior classification into the low (1 μM $ZnSO_4$) and high (10 mM $ZnSO_4$) treatment with a time component had an overall error-rate of 22.35%. Unlike *A. thaliana*, there was a higher percentage of Type II errors (36.4%) compared with Type I errors (8.3%).

Discussion

The FRET method has been used to monitor intracellular concentrations of various chemicals as they interact with cellular proteins (Miyawaki *et al.*, 1997; Hong and Maret, 2003; Abramoff *et al.*, 2004; Mattheyses *et al.*, 2004; Okumoto *et al.*, 2005). Only recently have these technologies been applied to plants (Kooshki *et al.*, 2003; Looger *et al.*, 2005; Deuschle *et al.*, 2006; Chen *et al.*, 2008a; Defraia *et al.*, 2008; Chaudhurri *et al.*, 2011). This new fusion of FRET technology with plant species has opened up the realm of biosensors. However, the use of FRET imaging at a whole-plant or tissue level to model anthropogenic substrates is severely limited.

In regard to the heavy-metal substrate in this study, plants have higher accumulation rates on soils with elevated Zn (Vandecasteele *et al.*, 2003; Adams *et al.*, 2011) lending themselves to real-time monitoring. Heavy metals such as Zn have specific avenues for plant entry and translocation through tissues leading to this increased accumulation. Here, we used one of these avenues, the Zn transporter (ZNT1), tandemly with the FRET concept to discriminate between low- and high-Zn treatments. We also demonstrated how this same construct can be used in various plant species.

We successfully produced chimeric plants by transforming the model plant species *A. thaliana* and the model forest species poplar. Both species containing the construct produced FRET changes as the plant interacted with increased presence of Zn. However, several lines from each transformation procedure are needed to obtain a functioning bio-sensor because the sequence for the chimeric protein is randomly inserted into the genome of the host. In functioning lines, observed changes in FRET (Table S1) can be attributed to the Zn gradient because other environmental conditions such as pH were held constant that would normally contribute to variation in the chimeric protein function (Chaudhuri *et al.*, 2008). As we would expect, leaf FRET activity in this study is not as quickly responsive as observed in previous studies using roots (Chaudhuri *et al.*, 2008) probably because nutrient translocation is not immediate (Adams *et al.*, 2011). However, given enough time for the Zn translocation into the leaf, which did occur by final harvest in this study (Table S4), FRET changes were able to be detected.

Changes in FRET do depend on the successful selection of a protein that has conformational changes when interacting with the desired substrate. This basic premise of FRET has been successfully harnessed to monitor substrates as they increase and decrease (Okumoto *et al.*, 2005). However, this does generally limit application to transport and binding proteins. In this study, we selected a protein that was shown in literature to interact with Zn (Pence *et al.*, 2000). While we did not know the specific native conformation of the protein and if the fusion of FPs to either termini would be spatially suitable for FRET, we selected this protein because it was relatively small (45.6 kDa) compared with other known Zn-interacting proteins such the 127.2 kDa protein HMA4 (Bernard *et al.*, 2004).

Functionality of the bio-sensor also depends on the activity of the FPs themselves. Past studies using FPs in plants have generally used a bioluminescence resonance energy transfer (BRET) strategy that substitutes a luciferase substrate in place of the FP donor (Xu *et al.*, 1999, 2007; Pfleger *et al.*, 2006; Xie *et al.*, 2011). This has allowed the FPs to be excited even if the external light cannot efficiently reach deeper tissues for excitation to occur (Xu *et al.*, 2007). In our construct, we used ECFP and DsRED that have been shown to work successfully *in vitro* as FRET partners (Erickson *et al.*, 2003; Kawai *et al.*, 2005; Zhang *et al.*, 2008). We must note, however, that DsRED has the major drawback of slow maturation, maturing from a light green phase to a red phase (Baird *et al.*, 2000; Mizuno *et al.*, 2001; Wiehler *et al.*, 2001; Labas *et al.*, 2002). This, in conjunction with our suboptimal microscope setting limitations, could potentially inhibit consistent FRET-based classification because of increased spectral cross-talk between FPs. Use of a DsRED variant with increased maturation rates could potentially increase bio-sensor precision of discrimination; however, our data demonstrate that DsRED and ECFP are adequate for producing FRET to discriminate largely differing Zn concentrations.

The model plant species *A. thaliana* is a small, annual plant and was a successful host for the PRZC construct with its relatively thin, young leaves with few trichomes and thin cuticle layer. However, for field deployment, the construct would eventually have to be put in a more practical plant based on features such as perennial growth habit, size and presence of evergreen leaves. Our study shows that application to different species does hold promise; however, we found two drawbacks when the system was transferred to and used in the tree species poplar that should be considered for future application into any species.

One potential drawback is differing leaf morphologies can dampen visualization. In this study, we used fully expanded leaves of both species for FRET visualization. Because of the life cycle differences of the two species, the mature leaves of poplar are older and thicker inhibiting penetration of the emitted light. This is critical as this light from the microscope needs to pass into the tissue where the proteins are located (Ruzin, 1999). This same feature will probably appear among species with year-long leaf retention. This would also be true if this construct were implemented into an evergreen such as *Pinus taeda* or *Quercus virginiana,* which also generally has a relatively thick cuticle layer. Because the cuticle layer is a major barrier against water loss in leaves, this added boundary that varies greatly among plants must be considered in the host plant (Riederer and Schreiber, 2001). Perhaps species with thicker tissues should be considered for the BRET strategy as previously mentioned.

A potential remedy to this problem, increasing the sensitivity of FRET visualization, may be the use of a different zinc transporter and/or promoter. *ZNT1* homologs have been shown to be located predominantly in the mesophyll and vascular bundle cells in other species (Pence *et al.*, 2000; Kupper *et al.*, 2007), while Zn has been shown to localize in both the mesophyll and epidermal cells (Migeon *et al.*, 2011). Use of a transporter that localizes in the epidermis and interacts with the Zn localizing in these cells would increase the sensitivity of our technique by

minimizing the physical distance that the lasers much penetrate into the tissue. This would then negate the problem of thickening leaves as they mature and may also alleviate problems posed by thick cuticle layers.

A second concern with our specific poplar clone is that it has extremely high amounts of trichomes adding to the three-dimensional shape and making resolution of the epidermal leaf surface difficult by diffracting light, preventing tissue penetration. In a laboratory setting, this could be overcome through removal of trichomes via a razor; however, intensive tissue preparation is not practical for low-impact field application. Alternatively, a simple solution would be selection of a poplar clone or other species with fewer trichomes to be the host for the PRZC construct. Acquisition of low-trichome plants is possible as there is a large genetic variation within species (Argen and Schemske, 1994; Valkama *et al.*, 2005).

Conclusions

Our findings show that *A. thaliana* as a host plant outperformed the same chimeric construct in poplar. Overall error-rates from discriminant analysis were similar between species, while Type I errors were substantially less in *A. thaliana*, lending itself to implementation with fewer false positives. Poplar does hold promise as a perennial alternative. However, the destination poplar clone had two drawbacks of greater leaf thickness and added dimensionality caused by dense trichomes. Such traits should be considered in the future when selecting a host for this FRET system. Still, the overall methods presented here demonstrate a biological method, in conjunction with current biotechnologies, for monitoring Zn accumulation in plants, serving as a bio-indicator of the local environment.

Experimental procedures

Fluorescent–protein fusion

We first searched for a target protein that was known to interact with Zn and to exhibit a conformational change upon interaction. The zinc transporter *ZNT1* gene was selected for use in this real-time monitoring system because the *Thlaspi caerulescens ZNT1* gene (*TcZNT1)* is a well studied member of the Zrt (Zinc Regulated Transporter), Irt (Iron Regulated Transporter)-like Protein (ZIP) family as a major component in Zn accumulation and transport in many species (Eng *et al.*, 1998; Guerinot, 2000; Pence *et al.*, 2000; Ramesh *et al.*, 2004; Antia *et al.*, 2006; Chiang *et al.*, 2006; Yang *et al.*, 2009). The poplar genome was queried for a *TcZNT1* homolog by blasting (i.e. blastp) the known *ZNT1* sequence from the hyper-accumulator *Thlaspi caerulescens* (AF133267) into the Phytozome v 5.0 database (http://www.phytozome.net/poplar.php), which includes the *Populus trichocarpa* genome v 2.0, and retrieving potential homologous sequences. Selection of a specific *P. trichocarpa* gene, *POPTR 0018s05190.1*, was based, in part, on the blastp score. The translated gene had a score of 426.0, while the next highest score was from gene *POPTR 0006s00860.1* with a score of 264.2. Supporting this was a phylogenetic analysis of potential poplar structural orthologs of *TcZNT1*. This was conducted by collecting transcript sequences, importing these into MEGA 4 (Tamura *et al.*, 2007), translating these into amino acid sequences, and aligning these with ClustalW (Thompson *et al.*, 1997) using the Gonnet protein weight matrix. Phylogenetic trees were generated from these alignments via the neighbor-joining method with bootstrapping (1000 replicates) and the maximum composite likelihood substitution model. The tree was rooted on a monocot [i.e. rice (*Oryza sativa*)] ortholog with ZIP annotation (Figure S1A). The translated *POPTR 0018s05190.1* gene aligned (Figure S1B) very closely to translated *TcZNT1* and *AtZIP4*, the *A. thaliana* homolog (Pence *et al.*, 2000; Assuncao *et al.*, 2001; Chen *et al.*, 2008b; Wu *et al.*, 2009).

PtZNT1 (*POPTR 0018s05190.1)* and its promoter (Pro_{PtZNT1}) were isolated from poplar. Total RNA was extracted from *P. trichocarpa* cv. Nisqually using the RNeasy Plant Mini Kit (Qiagen, Valencia, CA). One microgram of total RNA was reverse-transcribed using M-MLV reverse transcriptase (Promega, Madison, WI) to produce cDNA and used as a basis for transcript cloning. Poplar genomic DNA was extracted from leaf tissue using the DNeasy Plant Mini Kit (Qiagen) for use in promoter cloning. Forward and reverse primers were designed for the gene and promoter based on sequences from the poplar genome (Table S5). The gene sequence from cDNA was amplified with a three-step (94 °C-20 s, 50 °C-20 s, and 72 °C-150 s) 30-cycle programme using a PCR cocktail mixture of *Pfu* DNA-polymerase (Stratagene, La Jolla, CA), buffer and selected primers. The promoter sequence from genomic DNA was amplified using a three-step (94 °C-30 s, 55 °C-60 s and 72 °C-120 s) 30-cycle programme using an ex-*Taq* polymerase (Takara Bio Inc., Shiga, Japan), buffer and selected primers in a cocktail mixture. The amplicons were separated by electrophoresis on a 1% agarose gel, cloned into the pGEM-T Easy vector (Promega) and sequenced with CEQ 8000 Genetic Analysis System (Beckman-Coulter, Fullerton, CA). Additional terminal restriction site sequences (Table S5) were designed for each gene and added using a second PCR amplification reaction with the construct as the template, primer pairs (with added restriction sites) and *Pfu* DNA-polymerase in a PCR reaction. The altered gene was cloned into pGEM-T Easy vector and re-sequenced to ensure absence of sequence polymorphisms.

A red FP, *DsRed* (DsRed; BD Biosciences, San Diego, CA) and enhanced cyan FP, *ECFP* (Wang *et al.*, 2006), with absorption/emission peaks spectra of 558/583 and 434/477 nm, respectively, were used for fusion to *ZNT*. The promoter and gene were subcloned along with a red and cyan gene flanking the *ZNT* into the pUC19 vector. The new construct PRZC was then re-sequenced to ensure no premature translation terminations. A schematic of the chimaric construct is shown in Figure 1a. The PRZC construct was digested with appropriate enzymes and cloned into the binary vector pBI121 (Clontech, Palo Alto, CA) replacing both the cauliflower mosaic virus (CaMV) 35S constitutive expression promoter and the β-glucoronidase (*GUS*) reporter gene.

The PRZC construct was transformed into *Agrobacterium tumefaciens* C58, which subsequently was used to transform both wild-type *A. thaliana* (Col-0) and hybrid poplar clone INRA 717-1B4 (*Populus tremula* × *Populus alba*). *A. thaliana* and poplar transformation was performed using established transformation procedures (Han *et al.*, 2000; Clough, 2005). Independent lines of *A. thaliana* and poplar were initially screened with Kanamycin supplemented one-half Murashige and Skoog medium with 0.8% agar. *Arabidopsis thaliana* lines were also screened for five successive generations. Lines were then tested for transgene insertion through RT-PCR using

the red isolation (forward) primer and cyan reverse primer (Table S5). Ubiquitin (*UBQ*) amplification served as an internal control baseline. Positive transgenic lines from both species were randomly selected for metal challenges.

Fluorescent light emission was initially tested by subjecting plants to elevated Zn conditions (10 mM $ZnSO_4$) for 48 h. Wild-type (wt) plants and plants with *DsRED* under the CaMV 35S constitutive expression promoter (RED) were used as controls. Plants were harvested, washed, and leaf tissues were visualized for fluorescence using an Axiovert 200 M Inverted Research Microscope (Zeiss, Thornwood, NY) at the Mississippi State University Electron Microscope Center. Tissue was exposed to cyan and red excitation wavelengths (458/543 nm) via an Argon and HeNe laser simultaneously. The confocal microscope wavelength settings were not optimal; however, such settings have been previously employed while accepting some cross-excitation (Rizzo *et al.*, 2002). Emission light was viewed using each colour's respective filter (LP 475/BP560-615). Then, FRET activity was tested by exciting only the cyan fluorescence (458 nm) and using both filters.

FRET response in *Arabidopsis thaliana*

Three *A. thaliana* FRET-positive lines were selected for the metal assay based on an initial screening process. This screening included selection of plants that were positive for the chimeric gene, as indicated by RT-PCR, and that expressed a strong (relative to the other lines) cyan and red emission response when excited with both wavelengths. Lines and the controls were propagated and planted in 6.45-cm^2 pots containing sterile, inert sand. Each of the lines was tested using a 4 (rate) × 5 (sampling time) completely randomized design where 100 mL of $ZnSO_4$ was applied at four different rates as a supplement to the Hoagland's solution. All treatments were adjusted to pH 5.8 after addition of the Zn treatment. The four treatments consisted of the Hoagland's solution adjusted to 1 μM (control), 26 μM, 10 mM and 100 mM $ZnSO_4$. The second concentration, 26 μM Zn, was selected because it is the maximum concentration for sludge application allowed by the Environmental Protection Agency (EPA) (NRCS, 2000), providing a concentration which may be found in regular field type conditions. Four plants from each line were harvested at times 0, 1, 6, 24 and 48 h from each metal treatment. At harvest, plants were washed four times in ddH_2O and then mounted on a glass slide in a 50 μM saline solution.

DsRED and ECFP fusion proteins were activated and viewed with the Axiovert 200 M Inverted Research Microscope and a two-channel filter system composed of a BP 560–615-nm red spectrum and a LP 475-nm cyan spectrum. The microscope was first zeroed by exposing a wild-type plant from harvest time 0 to the excitation wavelength and adjusting the wavelength intensity so that tissue and slide auto-fluorescence was minimized. Following this calibration, three visualizations of the leaf of each plant were recorded for each of the three transgenic lines and control. These visualizations were saved as tiff image files and viewed using ImageJ 1.42 software (Abramoff *et al.*, 2004). In ImageJ, pictures were converted to Red, Blue, Green format and mean intensity of leaf and background areas for both cyan and red channelled pictures was measured. FRET was then calculated using Eqn. 1 for a two filter set protocol (Gordon *et al.*, 1998).

$$FRET = \frac{(Red_{\text{Tisssue}} - Red_{\text{Background}})}{(Cyan_{\text{Tissue}} - Cyan_{\text{Background}})} \quad (1)$$

Prior to statistical analysis, this FRET ratio was transformed with a log10 transformation. SAS 9.2 (SAS Institute Inc., 2008) was used to implement a general linear model in which metal concentration, time and metal concentration–time interaction were tested for effects on FRET by line. Changes in FRET were visualized three dimensionally over time and metal concentration using a script written in R which constructed an artificial independent variable grid with a range limit that included values actually used (R Development Core Team, 2008). Then, values were calculated for the given model and artificial independent values resulting in the three-dimensional visualization.

Metal concentration determination in *Arabidopsis thaliana*

Calculated FRET values from the three technical replications for each plant (*A. thaliana* assay #1) were averaged, and discriminate analysis was conducted at the biological replication level. Also, the classification groups were condensed in which treatment levels 1 μM (control) and 26 μM $ZnSO_4$ were considered low exposure and levels 1 mM and 10 mM $ZnSO_4$ were considered high exposure. This re-analysis used the discriminant function (Eqn. 2) in which coefficients '*a*' and '*b*' are listed in Table S3. This analysis only included data from 48 h because this was the time with the largest change over metal gradient (n = 12). A confusion matrix was used to assess classification success given the derived functions resulting in posterior probability error-rate, which is based on the posterior probabilities of the observations being classified in the same initial grouping.

$$Metal\ exposure = a + b\,Log(FRET) \quad (2)$$

A test for reproducibility of classification results was desired so an independent data set (n = 42) was generated from a second metal assay (*A. thaliana* assay #2) conducted with Line 3. Similar to the first assay, plants were grown for 2 weeks and then randomly assigned to either a control 1 μM $ZnSO_4$ or 10 mM $ZnSO_4$ application because classification success was maximized between the two extreme Zn concentrations. Each Zn treatment (100 mL) was applied at time 0, after the 48 h harvest and after the 96 h harvest. Three plants were harvested at 48, 72, 96 and 120 h. The application and harvest times were selected to expand the initial assay that was terminated at 48 h. After harvest, plants were washed, fixed on slides and visualized using previous procedures. FRET was calculated, and the data were tested at each time point independently using the previously derived discriminant functions.

Actual metal accumulation in *A. thaliana* leaf tissue was measured using established procedures for dry ash nutrient analysis (Isaac, 1983). Leaves of remaining plants were harvested at the conclusion of the assay, dried for 48 h at 50 °C and ground into a fine powder with a mortar and pestle. Two hundred milligrams of ground tissues were ashed at 500 °C for 4 h by placing ground tissues in a porcelain crucible in a furnace. Afterwards, samples were removed from the furnace and cooled to room temperature. Ash was gently mixed with 1 mL of hydrochloric acid and deionized water solution (1 : 1 v/v) and allowed to dissolve for 1 h. Subsequently, ash-containing liquid was successively decanted through 2 and 1-mm screens for 1 h, and the solution was collected. Leaf nutrient concentrations (zinc, calcium, potassium, magnesium, manganese, sodium, phosphorous, copper and iron mg/kg) were determined spectrophotometrically using an inductively coupled

plasma (ICP) emission spectrophotometer (Thermo Jarrel Ash Iris Advantage ICP, Houghton, MI).

FRET response and metal determination in poplar

Poplar plants representing four lines successfully expressing the PRZC construct were propagated in 39.5-cm^2 Magenta boxes (Plantmedia, Dublin, OH) with one-half strength Murashige and Skoog medium with 0.8% agar and grown till extensive root development (about 1 month). Afterwards, plants were transplanted into sterile, Pro-Mix® potting soil and grown for 1–2 months in 12.25-cm pots. These plants were extracted from the soil, washed and replanted into sterile, inert sand. Plants from each line were then grown in this medium for 6 day, and leaf samples from three independent plants were sampled. Based on *A. thaliana* metal assays, poplar samples were collected pretreatment (i.e. before application of Zn supplemented nutrient solution), at 72 h and at 120 h. Two treatments (1 μM ZnSO and 10 mM $ZnSO_4$) were applied at three times, which included after the first leaf samples were taken (0 h), 48 and 72 h after the leaf harvest. At each sampling time, leaf samples were taken from actively growing leaves on independent trees. Leaf tissues were washed four times in ddH_2O and then mounted on a glass slides in a 50 μM saline solution. Tissues that were visualized included six leaves from each of the four lines at each time point and metal treatment (n = 96) using methods described earlier. FRET was calculated, and a general linear model was used to test for metal effect on FRET, and changes of Line 3 FRET were visualized three-dimensionally over time and metal concentration as described earlier. Discriminant functions derived from *A. thaliana* data were first applied to test applicability of one interspecies set of functions. Then, an independent discriminant analysis was conducted on the poplar data using the function defined in Eqn. 3 in which coefficients '*a*', '*b*' and '*c*' are listed in Table S3. At the conclusion of the assay, metal accumulation from both metal treatments was measured using previous methods described for *A. thaliana*.

$$Metal\ exposure = a + b\,Log(FRET) + c(Days) \qquad (3)$$

Acknowledgements

We thank all of our student workers who have assisted at various times through the course of this project, most notably L. Vandervelde, M. Monroe and J. Ellis. We also would like to thank Dr. Thorsten Seidel (Bielefeld University) for his review of this manuscript during its preparation. This study was developed under a STAR Research Assistance Agreement No. FP916894 awarded by the Environmental Protection Agency. It has not been formally reviewed by the EPA. The views expressed in this study are solely the view of the authors and the EPA does not endorse any products or commercial services mentioned in this study.

The authors have declared no conflict of interest.

References

Abramoff, M.D., Megelhaes, P.J. and Ram, S.J. (2004) Image processing with ImageJ. *Biophotonics Int.* **11**, 36–42.

Adams, J.P., Adeli, A., Hsu, C.-Y., Harkess, R.L., Page, G.P., dePamphilis, C.W., Schultz, E.B. and Yuceer, C. (2011) Poplar maintains zinc homeostasis with heavy metal genes *HMA4* and *PCS1*. *J. Exp. Bot.* **62**, 3737–3752.

Allen, S.J., Hall, R.L. and Rosier, P.T.W. (1999) Transpiration by two poplar varities grown as coppice for biomass production. *Tree Physiol.* **19**, 493–501.

Antia, M., Islas, L.D., Boness, D.A., Baneyx, G. and Vogel, V. (2006) Single molecule fluorescence studies of surface-adsorbed fibronectin. *Biomaterials*, **27**, 679–690.

Argen, J. and Schemske, D.W. (1994) Evolution of trichome number in a naturalized population of *Brassica rapa*. *Am. Nat.* **143**, 1–13.

Assuncao, A., Da Costa Martins, P., De Folter, S., Vooijis, R., Schat, H. and Aarts, M. (2001) Elevated expression of metal transporter genes in three accessions of the metal hyperaccumulator *Thalspi caerulescens*. *Plant Cell Environ.* **24**, 217–226.

Baird, G.S., Zacharias, D.A. and Tsien, R.Y. (2000) Biochemistry, mutagenesis, and oligomerization of DsRed, a red fluorescent protein from coral. *Proc. Natl. Acad. Sci. USA*, **97**, 11984–11989.

Bernard, C., Roosens, N., Czernic, P., Lebrun, M. and Verbruggen, N. (2004) A novel CPx-ATPase from the cadmium hyperaccumulator *Thlaspi caerulescens*. *FEBS Lett.* **569**, 140–148.

Bojarczuk, K. (2004) Effect of toxic metals on the development of poplar (*Populus tremula* L. × *P. alba* L.) cultured *in vitro*. *Polish J. Environ. Stud.* **13**, 115–120.

Chaney, R.L. (1993) Zinc phytotoxicity. In *Zinc in Soils and Plants* (Robson, A.D., ed.), pp. 135–150. Dordrect: Kluwer Academic Publishing.

Chaudhuri, B., Hormann, F., Lalonde, S., Brady, S.M., Orlando, D.A., Benfey, P. and Frommer, W.B. (2008) Protonophore- and pH-insensitive glucose and sucrose accumulation detected by FRET nanosensors in *Arabidopsis* root tips. *Plant J.* **56**, 948–962.

Chaudhurri, B., Hormann, F. and Frommer, W.B. (2011) Dynamic imaging of glucose flux impedience using FRET sensors in wild-type *Arabidopsis* plants. *J. Exp. Bot.* **62**, 2411–2417.

Chen, H., Zou, Y., Shang, Y., Lin, H., Wang, Y., Cai, R., Tang, X. and Zhou, J.M. (2008a) Firefly luciferase complementation imaging assay for protein–protein interactions in plants. *Plant Physiol.* **146**, 368–376.

Chen, W.R., Feng, Y. and Chao, Y.E. (2008b) Genomic analysis and expression pattern of *OsZIP1, OsZIP3,* and *OsZIP4* in two rice *(Oryza sativaL.)* genotypes with differnt zinc efficiency. *Russ. J. Plant Physiol.* **55**, 400–409.

Chiang, H.C., Lo, J.C. and Yeh, K.C. (2006) Genes associated with heavy metal tolerance and accumulation in Zn/Cd hyperaccumulator *Arabidopsis halleri*: a genomic survey with cDNA microarray. *Environ. Sci. Technol.* **40**, 6792–6798.

Clough, S.J. (2005) Floral dip: *Agrobacterium*-mediated germ line transformation. *Methods Mol. Biol.* **286**, 91–102.

Cooper, D.T. and van Haverbeke, D. (1990) *Populus deltoides* Batr. ex Marsh eastern cottonwood. In *Silvics of North America: Hardwoods* (Burns, R.M. and Honkala, B.H., eds), pp. 530–543. Washington, DC: USDA Forest Service.

Defraia, C.T., Schmelz, E.A. and Mou, Z. (2008) A rapid biosensor-based method for quantification of free and glucose-conjugated salicylic acid. *Plant Methods*, **4**, 28.

DesRochers, A., van den Driessche, R. and Thomas, B.J. (2003) Nitrogen fertilization of trembling aspen grown on soils of different pH. *Can. J. For. Res.* **33**, 552–560.

Deuschle, K., Chaudhuri, B., Okumoto, S., Lager, I., Lalonde, S. and Frommer, W.B. (2006) Rapid metabolism of glucose detected with FRET glucose nanosensors in epidermal cells and intact roots of Arabidopsis RNA-silencing mutants. *Plant Cell*, **18**, 2314–2325.

Ebbs, S., Lau, I., Ahner, B. and Kochian, L. (2002) Phytochelatin synthesis is not responsible for Cd tolerance in the Zn/Cd hyperaccumulator *Thlaspi caerulescens* (J. & C. Presl). *Planta*, **214**, 635–640.

Eng, B.H., Guerinot, M.L., Eide, D. and Saier Jr, M.H. (1998) Sequence analyses and phylogenetic characterization of the ZIP family of metal ion transport proteins. *J. Membr. Biol.* **166**, 1–7.

Erickson, M.G., Moon, D.L. and Yue, D.T. (2003) DsRed as a potential FRET partner with CFP and GFP. *Biophys. J.* **85**, 599–611.

Gawel, J.E. and Hemond, H.F. (2004) Biomonitoring for metal contamination near two Superfund sites in Woburn, Massachusetts, using phytochelatins. *Environ. Pollut.* **131**, 125–135.

Gordon, G.W., Berry, G., Liang, X.H., Levine, B. and Herman, B. (1998) Quantitative fluorescence resonance energy transfer measurements using fluorescence microscopy. *Biophys. J.* **74**, 2702–2713.

Guerinot, M.L. (2000) The ZIP family of metal transporters. *Biochim. Biophys. Acta*, **1465**, 190–198.

Han, K.-H., Meilan, R., Ma, C. and Strauss, S.H. (2000) An *Agrobacterium tumefaciens* transformation protocol effective on variety of cottonwood hybrids (genus *Populus*). *Plant Cell Rep.* **19**, 315–320.

Hong, S.H. and Maret, W. (2003) A fluorescence resonance energy transfer sensor for the beta-domain of metallothionein. *Proc. Natl. Acad. Sci. USA*, **100**, 2255–2260.

Isaac, R. A. (1983) Reference Soil Test Methods for the Southern Region of the United States. Southern Cooperative Series Bulletin No. 289.

Kawai, H., Suzuki, T., Kobayashi, T., Sakurai, H., Ohata, H., Honda, K., Momose, K., Namekata, I., Tanaka, H., Shigenobu, K., Nakamura, R., Hayakawa, T. and Kawanishi, T. (2005) Simultaneous real-time detection of initiator- and effector-caspase activation by double fluorescence resonance energy transfer analysis. *J. Pharmacol. Sci.* **97**, 361–368.

Kooshki, M., Mentewab, A. and Stewart, C.N. (2003) Pathogen inducible reporting in transgenic tobacco using a GFP construct. *Plant Sci.* **165**, 213–219.

Kupper, H., Seib, L.O., Sivaguru, M., Hoekenga, O.A. and Kochian, L.V. (2007) A method for cellular localization of gene expression via quantitative *in situ* hybridization in plants. *Plant J.* **50**, 159–175.

Labas, Y.A., Gurskaya, N.G., Yanushevich, Y.G., Fradkov, A.F., Lukyanov, K.A., Lukyanov, S.A. and Matz, M.V. (2002) Diversity and evolution of the green fluorescent protein family. *Proc. Natl. Acad. Sci. USA*, **99**, 4256–4261.

Lager, I., Fehr, M., Frommer, W.B. and Lalonde, S. (2003) Development of a fluorescent nanosensor for ribose. *FEBS Lett.* **553**, 85–89.

Lakowicz, J.R. (ed.) (1999) *Principles of Fluorescence Spectroscopy*. New York, NY: Kluwer Academic/Plenum.

Li, J.A. and Brunner, A.M. (2009) Stability of transgenes in trees: expression of two reporter genes in poplar over three field seasons. *Tree Physiol.* **29**, 299–312.

Looger, L.L., Lalonde, S. and Frommer, W.B. (2005) Genetically encoded FRET sensors for visualizing metabolites with subcellular resolution in living cells. *Plant Physiol.* **138**, 555–557.

Mattheyses, A.L., Hoppe, A.D. and Axelrod, D. (2004) Polarized fluorescence resonance energy transfer microscopy. *Biophys. J.* **87**, 2787–2797.

Migeon, A., UAudinot, J.-N., Eybe, T., Richaud, P., Damien, B., Migeon, H.-N. and Chalot, M. (2011) Cadmium and zinc localization by SIMS in leaves of *Populus delotides* (cv.Lena) grown in a metal polluted soil. *Surf. Interface Anal.* **43**, 367–369.

Miyawaki, A., Llopis, J., Heim, R., McCaffery, J.M., Adams, J.A., Ikura, M. and Tsien, R.Y. (1997) Fluorescent indicators for Ca2+ based on green fluorescent proteins and calmodulin. *Nature*, **388**, 882–887.

Mizuno, H., Sawano, A., Eli, P., Hama, H. and Miyawaki, A. (2001) Red fluorescent protein from Discosoma as a fusion tag and a partner for fluorescence resonance energy transfer. *Biochemistry*, **40**, 2502–2510.

NRCS (2000) *Heavy Metal Soil Contamination*. Auburn, AL: United States Department of Agriculture.

Okumoto, S., Looger, L.L., Micheva, K.D., Reimer, R.J., Smith, S.J. and Frommer, W.B. (2005) Detection of glutamate release from neurons by genetically encoded surface-displayed FRET nanosensors. *Proc. Natl. Acad. Sci. USA*, **102**, 8740–8745.

Pence, N.S., Larsen, P.B., Ebbs, S.D., Letham, D.L., Lasat, M.M., Garvin, D.F., Eide, D. and Kochian, L.V. (2000) The molecular physiology of heavy metal transport in the Zn/Cd hyperaccumulator *Thlaspi caerulescens*. *Proc. Natl. Acad. Sci. USA*, **97**, 4956–4960.

Pfleger, K.D., Seeber, R.M. and Eidne, K.A. (2006) Bioluminescence resonance energy transfer (BRET) for the real-time detection of protein–protein interactions. *Nat. Protoc.* **1**, 337–345.

Podar, D., Ramsey, M.H. and Hutchings, M.J. (2004) Effect of cadmium, zinc and substrate heterogeneity on yield, shoot metal concentration and metal uptake by *Brassica juncea*: implications for human health risk assessment and phytoremediation. *New Phytol.* **163**, 313–324.

R Development Core Team (2008) *R: A Language and Environment for Statistical Computing*. Vienna, Austria: R Foundataion for Statistical Computing.

Ramesh, S.A., Choimes, S. and Schachtman, D.P. (2004) Over-expression of an *Arabidopsis* zinc transporter in *Hordeum vulgare* increases short-term zinc uptake after zinc deprivation and seed zinc content. *Plant Mol. Biol.* **54**, 373–385.

Riederer, M. and Schreiber, L. (2001) Protecting against water loss: analysis of the barrier properties of plant cuticles. *J. Exp. Bot.* **52**, 2023–2032.

Rizzo, M.A., Magnuson, M.A., Drain, P.F. and Piston, D.W. (2002) A functional link between glucokinase binding to insulin granules and conformational alterations in response to glucose and insulin. *J. Biol. Chem.* **277**, 34168–34175.

Ruzin, S.E. (ed.) (1999) *Plant Microtechnique and Microscopy*. New York: Oxford University Press.

Sanyal, A., Rautaray, D., Bansal, V., Ahmad, A. and Sastry, M. (2005) Heavy-metal remediation by a fungus as a means of production of lead and cadmium carbonate crystals. *Langmuir*, **21**, 7220–7224.

SAS Institute Inc (2008) *SAS 9.2*. Cary, NC: SAS Institute Inc.

Tamura, K., Dudley, J., Nei, M. and Kumar, S. (2007) MEGA4: molecular evolutionary genetics analysis (MEGA) software version 4.0. *Mol. Biol. Evol.* **24**, 1596–1599.

Thompson, J.D., Gibson, T.J., Plewniak, F., Jeanmougin, F. and Higgins, D.G. (1997) The CLUSTAL_X windows interface: flexible strategies for multiple sequence alignment aided by quality analysis tools. *Nucleic Acids Res.* **25**, 4876–4882.

Valkama, E., Koricheva, J., Salminen, J.-P., Helander, M., Saloniemi, I., Saikkonen, K. and Pihlaja, K. (2005) Leaf surface traits: overlooked determinants of birch resistance to herbivores and foliar micro-fungi? *Trees.* **19**, 191–197.

Vandecasteele, B., Lauriks, R., De Vos, B. and Tack, F.M. (2003) Cd and Zn concentration in hybrid poplar foliage and leaf beetles grown on polluted sediment-derived soils. *Environ. Monit. Assess.* **89**, 263–283.

Vervaeke, P., Luyssaert, S., Mertens, J., Meers, E., Tack, F.M. and Lust, N. (2003) Phytoremediation prospects of willow stands on contaminated sediment: a field trial. *Environ. Pollut.* **126**, 275–282.

Vinkenborg, J.L., Nicolson, T.J., Bellomo, E.A., Koay, M.S., Rutter, G.A. and Merkx, M. (2009) Genetically encoded FRET sensors to monitor intracellular Zn2+ homeostasis. *Nat. Methods*, **6**, 737–740.

Wang, D., Tyson, M.D., Jackson, S.S. and Yadegari, R. (2006) Partially redundant functions of two SET-domain polycomb-group proteins in controlling initiation of seed development in *Arabidopsis*. *Proc. Nat. Acad. Sci. USA*, **103**, 13244–13249.

Watson, R., Nobel, I., Bolin, B., Ravindranath, N., Verardo, D. and Dokken, D. (eds) (2000) *Land Use, Land-Use Change, and Forestry*. Cambridge, UK: Cambridge University Press.

Wiehler, J., von Hummel, J. and Steipe, B. (2001) Mutants of Discosoma red fluorescent protein with a GFP-like chromophore. *FEBS Lett.* **487**, 384–389.

Wu, J., Zhao, F.J., Ghandilyan, A., Brabara, L., Guzman, M.O., Schat, H., Wang, X. and Aarts, M. (2009) Identification and functional analysis of two ZIP metal transporters of the hyperaccumulator *Thlaspi caerulescens*. *Plant Soil*, **325**, 79–95.

Xie, Q., Soutto, M., Xu, X., Zhang, Y. and Johnson, C.H. (2011) Bioluminescence resonance energy transfer (BRET) imaging in plant seedlings and mammalian cells. *Methods Mol. Biol.* **680**, 3–28.

Xu, Y., Piston, D.W. and Johnson, C.H. (1999) A bioluminescence resonance energy transfer (BRET) system: application to interacting circadian clock proteins. *Proc. Nat. Acad. Sci. USA*, **96**, 151–156.

Xu, X., Soutto, M., Xie, Q., Servick, S., Subramanian, C., von Arnim, A.G. and Johnson, C.H. (2007) Imaging protein interactions with bioluminescence resonance energy transfer (BRET) in plant and mammalian cells and tissues. *Proc. Nat. Acad. Sci. USA*, **104**, 10264–10269.

Yang, X., Huang, J., Jiang, Y. and Zhang, H.S. (2009) Cloning and functional identification of two members of the ZIP (Zrt, Irt-like protein) gene family in rice (*Oryza sativa* L.). *Mol. Biol. Rep.* **36**, 281–287.

Yang, H., Bogner, M., Stierhof, Y.D. and Ludewig, U. (2010) H-independent glutamine transport in plant root tips. *PLoS ONE*, **5**, e8917.

Zhang, Z., Yang, J., Lu, J., Lin, J., Zeng, S. and Luo, Q. (2008) Fluorescence imaging to assess the matrix metalloproteinase activity and its inhibitor *in vivo*. *J. Biomed. Opt.* **13**, 011006.

Supporting information

Additional supporting information may be found in the online version of this article:

Figure S1 (A) Potential poplar ortholog, *POPTR 0018s05190.1*, was identified from a phylogenetic tree based on relationship to *TcZNT*, *AtZIP4*, and *OsZIP* from species *Thlaspi caerulescens*, *A. thaliana*, and *Oryza sativa*, respectively. (B) The amino acid alignment created with ClustalW is displayed between the selected poplar ortholog, *POPTR 0018s05190.1*, and *TcZNT1* and *AtZIP4*.

Table S1 Normalized FRET intensities produced from leaf tissue from two independent *Arabidopsis thaliana* assays and one poplar assay using various Zn concentrations and harvest times after Zn application.

Table S2 Discriminant function coefficients based on measured FRET values from *Arabidopsis thaliana* and poplar leaf tissues.

Table S3 Confusion matrices from discriminant functions derived from *A. thaliana* and poplar lines' FRET values between high and low Zn levels.

Table S4 Leaf nutrient accumulation mean and variance across two Zn treatments (1 μM and 10 mM) in *Arabidopsis thaliana* and poplar.

Table S5 Primer list for poplar gene, promoter, and fluorescent gene isolation, cloning, and confirmation.

Please note: Wiley-Blackwell are not responsible for the content or functionality of any supporting materials supplied by the authors. Any queries (other than missing material) should be directed to the corresponding author for the article.